

Chapter 5

Delay Differential Equations

5.1 Preliminary Examples

5.1.1 Numerical Solutions

We start by considering a pair of delay differential equations:

$$y'(t) = ay(t)(1 - y(t - \tau)) \quad (5.1)$$

and

$$y'(t) = \frac{by(t - \tau)}{1 + [y(t - \tau)]^n} - ay(t). \quad (5.2)$$

The numerical solutions to these are graphed in figures 5.1–5.4.

5.1.2 Region of Stability of a Simple Example

Consider the stability of the zero solution of

$$y'(t) = ay(t) + by(t - 1). \quad (5.3)$$

Let

$$y = \epsilon e^{\lambda t}. \quad (5.4)$$

Then

$$\lambda = a + be^{-\lambda}. \quad (5.5)$$

If we let $\lambda = p + iq$, then we obtain that

$$p = a + be^{-p} \cos(q) \quad (5.6)$$

$$q = -be^{-p} \sin(q) \quad (5.7)$$

so that

$$\frac{p - a}{q} = -\cot(q) \quad (5.8)$$

$$p = a - q \cot(q). \quad (5.9)$$

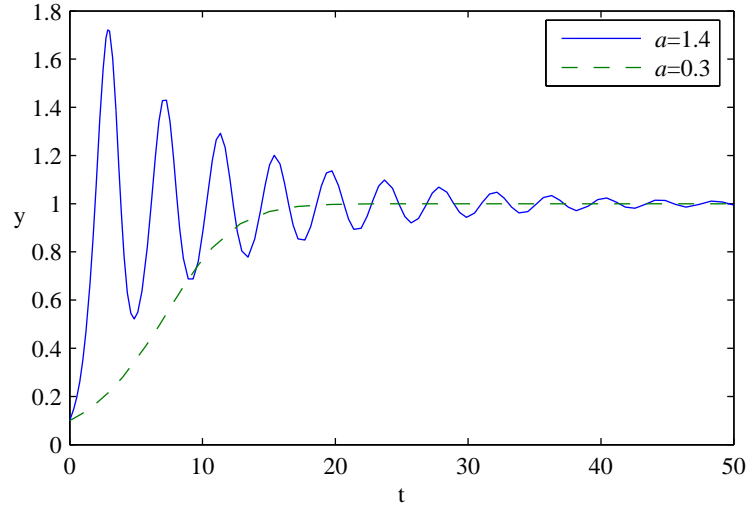


Figure 5.1: The solution of equation 5.1 with $y(t) = 0.1$ for $t \leq 0$ and $\tau = 1$.

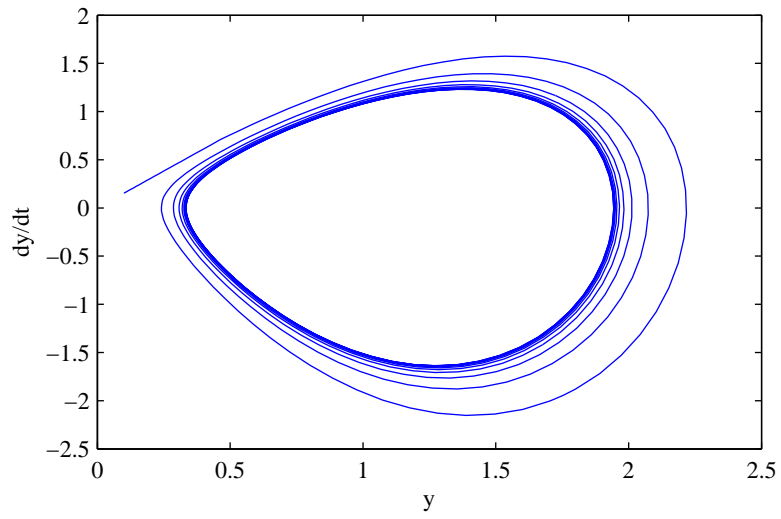


Figure 5.2: The solution of equation 5.1 with $y(t) = 0.1$ for $t \leq 0$, $\tau = 1$ and $a = 1.7$ in the phase plane.

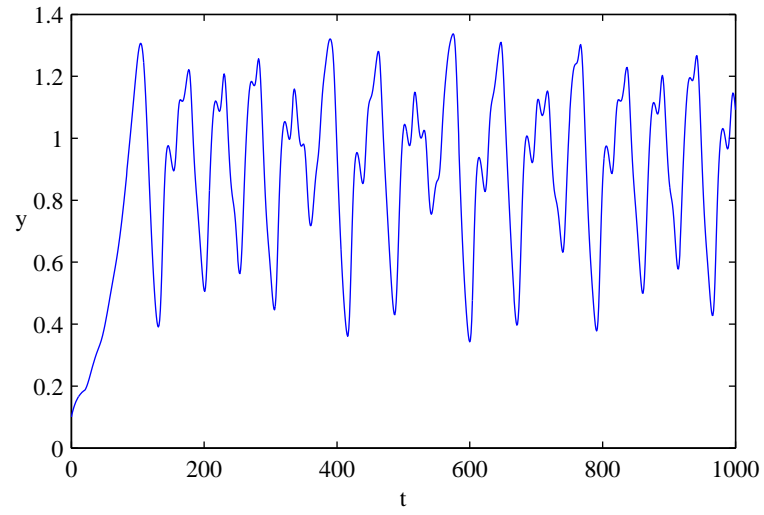


Figure 5.3: The solution of equation 5.2 with $y(t) = 0.1$ for $t \leq 0$, $\tau = 20$, $a = 0.1$, $b = 0.2$ and $n = 10$.

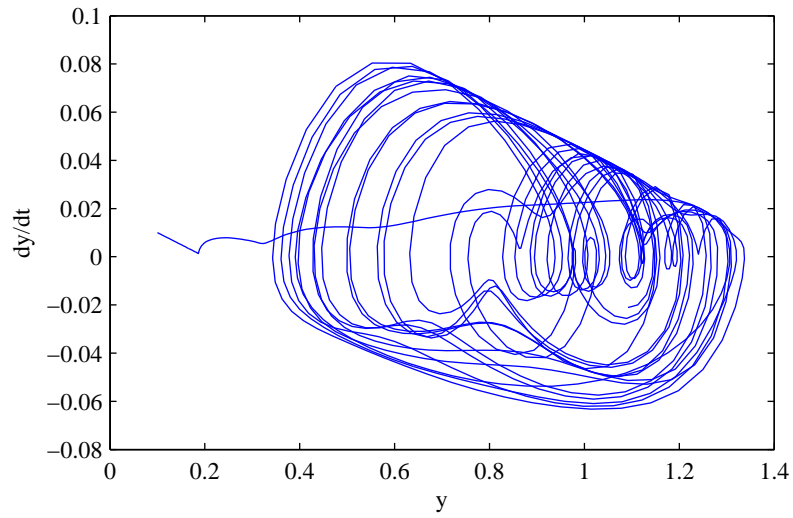


Figure 5.4: The solution of equation 5.2 with $y(t) = 0.1$ for $t \leq 0$, $\tau = 20$, $a = 0.1$, $b = 0.2$ and $n = 10$ in the phase plane.

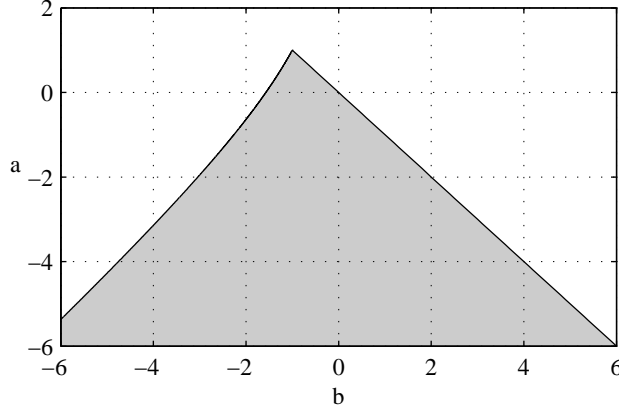


Figure 5.5: The region of stability of the zero solution of equation 5.3, as a function of a and b .

Now if the zero solution is unstable, there must exist some λ such that $p > 0$, which means that

$$a > q \cot(q). \quad (5.10)$$

Also,

$$q = -be^{-p} \sin(q) \quad (5.11)$$

$$e^{-p} = \frac{-q}{b \sin(q)} \quad (5.12)$$

so in order to have $p > 0$, we must also have

$$0 < \frac{-q}{b \sin(q)} < 1. \quad (5.13)$$

Now these assumed that $q \neq 0$, so that $b \neq 0$ and $\sin(q) \neq 0$. If $q = 0$, we obtain that

$$a = p - be^{-p}, \quad (5.14)$$

where this gives instability for $p > 0$. Solving equations 5.10, 5.13 and 5.14 numerically, we obtain the plot shown in figure 5.5. Note that figure 5.5 is slightly different from the figure presented by Qian [22], although figure 5.5 agrees with that on p.56 of El'sgol'ts [6]. As confirmation of our depiction of the region of stability, we numerically compute some solutions to equation 5.3. These are shown in figure 5.6. Note that for $a = 0, b = 1$, Qian [22] predicts stability, whereas it can be seen in figure 5.6 that we obtain instability. This corresponds to the special case when $q = 0$, as in equation 5.14.

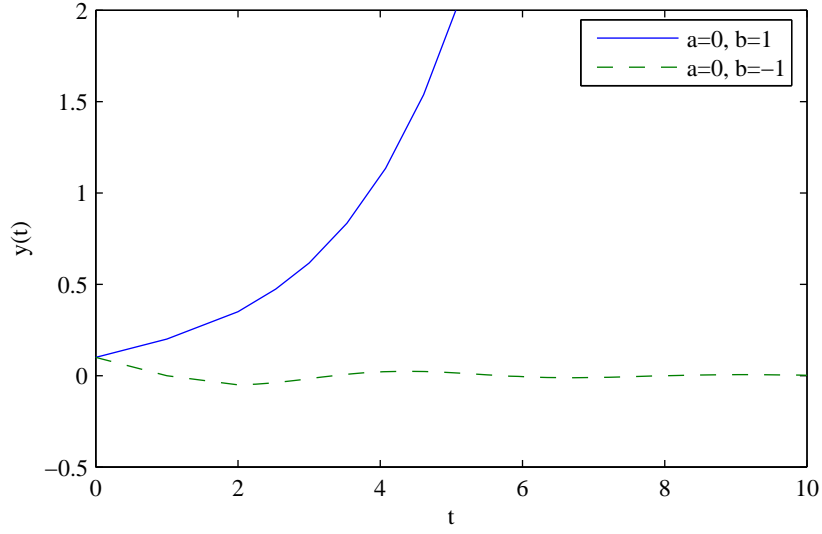


Figure 5.6: Some solutions to equation 5.3, with $y(t) = 0.1$ for $t < 0$.

Lyapunov function

Following Qian [22], we define a Lyapunov function

$$L[y(t)] = y^2(t) + |b| \int_{t-1}^t y^2(s) ds, \quad (5.15)$$

which satisfies $L \geq 0$. Also observe that

$$0 \leq |b| (y(t) - y(t-1))^2 \quad (5.16)$$

$$2|b| y(t)y(t-1) \leq |b| (y^2(t) + y^2(t-1)) \quad (5.17)$$

$$2by(t)y(t-1) \leq |b| (y^2(t) + y^2(t-1)) \quad (5.18)$$

so that

$$\frac{dL}{dt} = 2y(t)y'(t) + |b| (y^2(t) - y^2(t-1)) \quad (5.19)$$

$$= 2y(ay(t) + by(t-1)) + |b| (y^2(t) - y^2(t-1)) \quad (5.20)$$

$$= 2ay^2(t) + 2by(t)y(t-1) + |b| (y^2(t) - y^2(t-1)) \quad (5.21)$$

$$\leq 2ay^2(t) + |b| (y^2(t) + y^2(t-1)) + |b| (y^2(t) - y^2(t-1)) \quad (5.22)$$

$$\leq 2(a + |b|) y^2(t) \quad (5.23)$$

which is negative for $a + |b| \leq 0$. As a result, $a \leq -|b|$ is a sufficient condition for stability. Observe that this region is contained within the region of stability shown in figure 5.5.

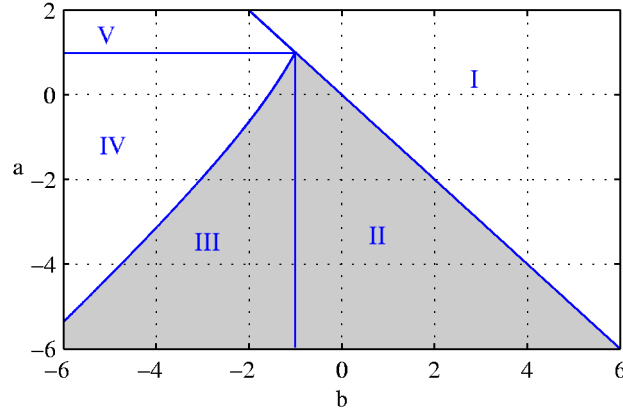


Figure 5.7: The different regions used for the Nyquist proof of stability, with the region of stability shaded as in figure 5.5.

Nyquist theorem

We wish to prove that the shaded region in figure 5.7 is indeed stable and that the unshaded region is unstable.

Let

$$f(\lambda) = \lambda - a - be^{-\lambda}. \quad (5.24)$$

Then the eigenvalues are the roots of $f(\lambda) = 0$. Let C_R be a semicircular curve in the right half of the complex plane from $-iR$ through R to iR , and let Γ_I be a line in the complex plane from iR to the origin. Then

$$\lim_{R \rightarrow \infty} (\Delta_{C_R} \arg(f(\lambda)) + 2\Delta_{\Gamma_I} \arg(f(\lambda))) = 2\pi N \quad (5.25)$$

where N is the number of zeroes in the right half plane. Observe that

$$\lim_{R \rightarrow \infty} \Delta_{C_R} \arg(f(\lambda)) = \pi \quad (5.26)$$

since

$$f(\lambda) = \lambda \left(1 - \frac{a + be^{-\lambda}}{\lambda} \right). \quad (5.27)$$

Now consider the value of $f(\lambda)$ along Γ_I . Let $\lambda = i\lambda_I$ so that

$$f(\lambda) = (-a - b \cos(\lambda_I)) + i(\lambda_I + b \sin(\lambda_I)) \quad (5.28)$$

$$\equiv f_R + if_I. \quad (5.29)$$

Observe that

$$\lim_{R \rightarrow \infty} \arg(f(iR)) = \frac{\pi}{2} \quad (5.30)$$

since $f_I \rightarrow \infty$ but f_R remains finite. Now consider the different regions presented in figure 5.7.

I. In this region, $a > -b$, so $\arg(f(0)) = \pi$. As a result,

$$\lim_{R \rightarrow \infty} \Delta_{\Gamma_I} \arg(f(\lambda)) = \frac{\pi}{2} + 2\pi k, \quad k \in \mathbb{Z} \quad (5.31)$$

so equation 5.25 becomes

$$\pi + 2 \left(\frac{\pi}{2} + 2\pi k \right) = 2\pi N \quad (5.32)$$

$$2\pi(1 + 2k) = 2\pi N. \quad (5.33)$$

Since N by definition must be at least 0, equation 5.33 tells us that N is at least 1, so the solution is unstable in this region.

II. In this region, $a < -b$ and $b > -1$. Since $a < -b$, $\arg(f(0)) = 0$. We will start by proving that for no λ_I can we simultaneously have $f_I = 0$ and $f_R < 0$.

If $f_R < 0$, then

$$-a - b \cos(\lambda_I) < 0, \quad (5.34)$$

so

$$a > -b \cos(\lambda_I). \quad (5.35)$$

But since $-b < a$, then

$$-b > -b \cos(\lambda_I). \quad (5.36)$$

Note that if $b > 0$, we would get $1 < \cos(\lambda_I)$, a contradiction, and so we must have $b < 0$. As a result, if $f_I = 0$, then

$$\lambda_I + b \sin(\lambda_I) = 0 \quad (5.37)$$

and so $b < 0$ means

$$b = \frac{-\lambda_I}{\sin(\lambda_I)} < 0. \quad (5.38)$$

Since $\lambda_I > 0$ by definition, this means that $\sin(\lambda_I) > 0$. Also, since $b > -1$, this means

$$b = \frac{-\lambda_I}{\sin(\lambda_I)} > -1, \quad (5.39)$$

and so since $\sin(\lambda_I) > 0$,

$$\frac{\lambda_I}{\sin(\lambda_I)} < 1 \quad (5.40)$$

$$\lambda_I < \sin(\lambda_I), \quad (5.41)$$

which is a contradiction for $\lambda_I > 0$.

As a result, we can never simultaneously have $f_I = 0$ and $f_R < 0$ in this region, so

$$\lim_{R \rightarrow \infty} \Delta_{\Gamma_I} \arg(f(\lambda)) = -\frac{\pi}{2} \quad (5.42)$$

and hence equation 5.25 tells us there are no eigenvalues in the right half plane, and so the solution is stable in this region.

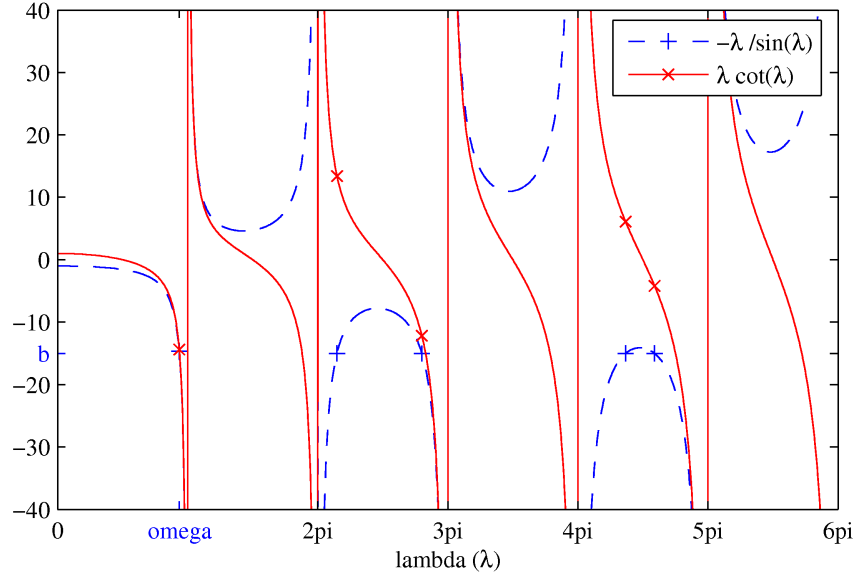


Figure 5.8: An illustration used in showing that in case III, if $f_I = 0$, we must have $f_R > 0$. See text.

III. In this region, there is some ω such that $b = -\omega / \sin(\omega)$, $a < \omega \cot(\omega)$. Now if $f_I = 0$, then

$$b = -\frac{\lambda_I}{\sin(\lambda_I)}. \quad (5.43)$$

Now $\lambda_I = \omega$ satisfies the above equation and since $a < \omega \cot(\omega)$, then

$$-b \cos(\omega) > a \quad (5.44)$$

$$f_R > 0. \quad (5.45)$$

We wish to show that in fact for any λ^* such that $f_I(\lambda^*) = 0$, we must have $f_R(\lambda^*) > 0$. We direct the reader's attention to figure 5.8. Observe that for all $\lambda^* > \omega$ such that $-\omega / \sin(\omega) = -\lambda^* / \sin(\lambda^*)$ (i.e., $f_I(\lambda^*) = 0$) marked by blue + signs, that $\lambda^* \cot(\lambda^*) > \omega \cot(\omega)$ marked by red x signs. As a result, since $a < \omega \cot(\omega)$ we must also have $a < \lambda^* \cot(\lambda^*)$ and hence, $f_R(\lambda^*) > 0$. We then conclude that whenever $f_I = 0$, we must have $f_R > 0$, and so

$$\lim_{R \rightarrow \infty} \Delta_{\Gamma_I} \arg(f(\lambda)) = -\frac{\pi}{2} \quad (5.46)$$

and hence equation 5.25 tells us that the solution is stable in this region.

IV. In this region, there is some ω such that $b = -\omega/\sin(\omega)$, $a > \omega \cot(\omega)$, and $a < 1$. This means that

$$\omega + b \sin(\omega) = 0 \quad (5.47)$$

$$f_I(\omega) = 0 \quad (5.48)$$

and

$$\frac{\omega \cos(\omega)}{\sin(\omega)} < a \quad (5.49)$$

$$-b \cos(\omega) < a \quad (5.50)$$

$$-a - b \cos(\omega) < 0 \quad (5.51)$$

$$f_R(\omega) < 0. \quad (5.52)$$

Now observe that, in general, if $f_R < 0$,

$$a + b \cos(\lambda_I) > 0 \quad (5.53)$$

and so if $a < 1$,

$$1 + b \cos(\lambda_I) > 0 \quad (5.54)$$

$$\frac{df_I}{d\lambda_I} > 0. \quad (5.55)$$

So as λ_I decreases from infinity to zero, if $f_R < 0$, then f_I can only decrease. As a result, since we have from above that there is some $\lambda_I = \omega$ such that $f_R < 0$ and $f_I = 0$, then we must have

$$\lim_{R \rightarrow \infty} \Delta_{\Gamma_I} \arg(f(\lambda)) \geq \frac{3\pi}{2}. \quad (5.56)$$

Equation 5.25 then tells us that our solution is unstable in this region.

V. In this region, $a < -b$, $b < -1$ and $a > 1$. From figure 5.9, it is evident that for $0 < c < 1$,

$$(\cos^{-1}(c))^2 + \left(1 - \frac{1}{c^2}\right) \leq 0. \quad (5.57)$$

Now for $0 < c < 1$, we have that $1 - 1/c^2 < 0$ and so for $a > 1$,

$$a^2 \left(1 - \frac{1}{c^2}\right) < \left(1 - \frac{1}{c^2}\right) \quad (5.58)$$

$$(\cos^{-1}(c))^2 + a^2 \left(1 - \frac{1}{c^2}\right) < 0 \quad (5.59)$$

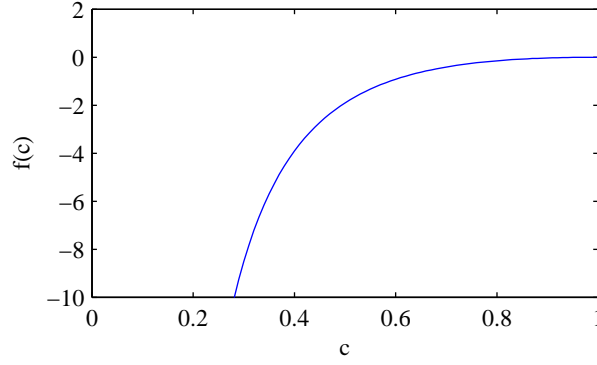


Figure 5.9: The function in equation 5.57, showing that it's negative everywhere for $0 < c < 1$.

Observe that since $a < -b$ and $b < 0$, then $-a/b < 1$ and since $a > 0$, $b < 0$, then $-a/b > 0$. We can then choose to let $c = -a/b$. We obtain

$$\left(\cos^{-1}\left(\frac{a}{-b}\right)\right)^2 + a^2 - b^2 < 0 \quad (5.60)$$

$$\left(\cos^{-1}\left(\frac{a}{-b}\right)\right)^2 < b^2 - a^2 \quad (5.61)$$

and since $0 < a < -b$, $0 < b^2 - a^2$, and so

$$\cos^{-1}\left(\frac{a}{-b}\right) < \sqrt{b^2 - a^2} \quad (5.62)$$

$$\cos^{-1}\left(\frac{a}{-b}\right) + b \frac{\sqrt{b^2 - a^2}}{-b} < 0. \quad (5.63)$$

Now let $\lambda^* = \cos^{-1}(a/-b)$ so that $f_R(\lambda^*) = 0$ and

$$\lambda^* + b \sin(\lambda^*) < 0 \quad (5.64)$$

$$f_I(\lambda^*) < 0. \quad (5.65)$$

Now observe that, in general, if $f_I < 0$,

$$\lambda_I + b \sin(\lambda_I) < 0 \quad (5.66)$$

$$b \sin(\lambda_I) < -\lambda_I \quad (5.67)$$

$$b \sin(\lambda_I) < 0 \quad (5.68)$$

$$\frac{df_R}{d\lambda_I} < 0. \quad (5.69)$$

As a result, if $f_I < 0$, as λ_I decreases from infinity to zero, f_R must be increasing. Since we have found a $\lambda_I = \lambda^*$ such that $f_R = 0$ and $f_I < 0$, then we must have

$$\lim_{R \rightarrow \infty} \Delta_{\Gamma_I} \arg(f(\lambda)) \geq \frac{3\pi}{2}. \quad (5.70)$$

Equation 5.25 then tells us that our solution is unstable in this region.

We have then proved the different regions of stability and instability as shown in figure 5.7.

5.2 Machine Tool Vibrations

Consider the following model of turning from St'ep'an et al. [26]. We set up our model such that the blade will, in theory, continuously cut a depth h_0 and a width w . Suppose our turning mechanism turns the workpiece with period τ . Then the actual depth cut by the blade at time t is

$$h(t) = h_0 + x(t - \tau) - x(t), \quad (5.71)$$

where x corresponds to how much the material was under/ over cut. For example, if x is positive, then the material was not cut deep enough. The force on the blade is

$$F_x = Kwh^{3/4}, \quad (5.72)$$

so the added force on the blade due to the cutting irregularities is

$$\Delta F_x = Kw(h_0 + x(t - \tau) - x(t))^{3/4} - Kw h_0^{3/4}. \quad (5.73)$$

Expanding this as a Taylor series about $x(t - \tau) - x(t)$, we obtain

$$\begin{aligned} \Delta F_x &= Kw \frac{3}{4} h_0^{-1/4} (x(t - \tau) - x(t)) \\ &\quad - Kw \frac{1}{2!} \cdot \frac{3}{4} \cdot \frac{1}{4} h_0^{-5/4} (x(t - \tau) - x(t))^2 \\ &\quad + Kw \frac{1}{3!} \cdot \frac{3}{4} \cdot \frac{1}{4} \cdot \frac{5}{4} h_0^{-9/4} (x(t - \tau) - x(t))^3. \end{aligned} \quad (5.74)$$

Letting

$$k_1 = \frac{Kw}{\sqrt[4]{h_0}} \frac{3}{4}, \quad (5.75)$$

this becomes

$$\begin{aligned} \Delta F_x &= k_1 (x(t - \tau) - x(t)) - \frac{k_1}{8h_0} (x(t - \tau) - x(t))^2 \\ &\quad + \frac{5k_1}{96h_0^2} (x(t - \tau) - x(t))^3. \end{aligned} \quad (5.76)$$

This force goes into moving the tool, and is absorbed by damping in the tool and the spring constant of the tool, so that

$$\Delta F_x = m\ddot{x} + b\dot{x} + kx, \quad (5.77)$$

where m is the mass, b is the damping coefficient and k is the spring constant. To check that all the signs are correct in the above equation, consider the following simple cases:

- i. If $b = 0$, $k = 0$ and $\Delta F_x > 0$, which means we're currently cutting deeper than the tool likes, we will get $m\ddot{x} > 0$, so x will increase and we will start to cut shallower.
- ii. If $F_x = 0$, $k = 0$ and $\dot{x} > 0$, then we will get $\ddot{x} < 0$, which is the damping effect that we expect.
- iii. If $F_x = 0$, $b = 0$ and $x > 0$, then we will get $\ddot{x} < 0$, which is the effect that we expect the spring to have.

So we obtain that

$$\begin{aligned} k_1 (x(t - \tau) - x(t)) - \frac{k_1}{8h_0} (x(t - \tau) - x(t))^2 + \frac{5k_1}{96h_0^2} (x(t - \tau) - x(t))^3 \\ = m\ddot{x} + b\dot{x} + kx. \end{aligned} \quad (5.78)$$

Letting $p = k_1/k$ and $\zeta = b/(2\sqrt{km})$, this becomes

$$\begin{aligned} k (x(t - \tau) - x(t)) - \frac{k}{8h_0} (x(t - \tau) - x(t))^2 + \frac{5k}{96h_0^2} (x(t - \tau) - x(t))^3 \\ = \frac{m}{k} \ddot{x} + 2\zeta \sqrt{\frac{m}{k}} \dot{x} + x. \end{aligned} \quad (5.79)$$

Now we let $\tilde{t} = t\sqrt{k/m}$ and $\tilde{\tau} = \tau\sqrt{k/m}$, where $\sqrt{k/m}$ is the resonant frequency of the tool, so that

$$x' = \dot{x} \sqrt{\frac{m}{k}}, \quad x'' = \ddot{x} \frac{m}{k}, \quad (5.80)$$

where dot denotes differentiation with respect to t and prime denotes differentiation with respect to \tilde{t} . Then

$$\begin{aligned} x'' + 2\zeta x' + (1 + p)x(\tilde{t}) - p(x(\tilde{t} - \tilde{\tau})) = \frac{-p}{8h_0} (x(\tilde{t} - \tilde{\tau}) - x(\tilde{t}))^2 \\ + \frac{5p}{96h_0^2} (x(\tilde{t} - \tilde{\tau}) - x(\tilde{t}))^3 \end{aligned} \quad (5.81)$$

For simplicity of the model, we choose h_0 such that $1/8h_0 = 5/96h_0^2$. Then we finally have our non-dimensionalised model for machine tool vibrations:

$$\boxed{x'' + 2\zeta x' + (1 + p)x - px_\tau = -\frac{3p}{10} \left((x_\tau - x)^2 - (x_\tau - x)^3 \right)} \quad (5.82)$$

where $x = x(\tilde{t})$ and $x_\tau \equiv x(\tilde{t} - \tilde{\tau})$. Approximating this near the zero solution by

$$x(t) = ce^{\lambda \tilde{t}}, \quad (5.83)$$

we obtain, as in the paper by Stépán et al. [26], that

$$\lambda^2 + 2\zeta\lambda + (1 + p) - pe^{-\tilde{\tau}\lambda} = 0. \quad (5.84)$$

To determine the stability boundary, we let $\lambda = \pm i\omega$. Without loss of generality, we can choose the positive sign. Following Ward [28], we obtain that

$$-\omega^2 + 2i\omega\zeta + (1 + p) - p(\cos(\tilde{\tau}\omega) - i\sin(\tilde{\tau}\omega)) = 0. \quad (5.85)$$

Equating real and imaginary parts, this becomes

$$-\omega^2 + 1 = p(\cos(\tilde{\tau}\omega) - 1) \quad (5.86)$$

$$-2\omega\zeta = p\sin(\tilde{\tau}\omega), \quad (5.87)$$

so that

$$(1 - \omega^2)^2 + 2p(1 - \omega^2) + p^2 + 4\omega^2\zeta^2 = p^2 \quad (5.88)$$

$$\frac{(1 - \omega^2)^2 + 4\omega^2\zeta^2}{2(\omega^2 - 1)} = p. \quad (5.89)$$

Since $p > 0$ from the physical quantities it's defined by, we then conclude that $\omega > 1$. Returning to equations 5.86 and 5.87, we obtain that

$$\frac{1 - \cos(\tilde{\tau}\omega)}{\sin(\tilde{\tau}\omega)} = \frac{\omega^2 - 1}{-2\omega\zeta} \quad (5.90)$$

$$\frac{2\sin^2(\omega\tilde{\tau}/2)}{2\sin(\omega\tilde{\tau}/2)\cos(\omega\tilde{\tau}/2)} = \frac{\omega^2 - 1}{-2\omega\zeta} \quad (5.91)$$

$$\tan\left(\frac{\omega\tilde{\tau}}{2}\right) = \frac{\omega^2 - 1}{-2\omega\zeta} \quad (5.92)$$

$$\frac{\omega\tilde{\tau}}{2} = \tan^{-1}\left(\frac{\omega^2 - 1}{-2\omega\zeta}\right) + j\pi \quad (5.93)$$

$$\tilde{\tau} = \frac{2}{\omega} \left(j\pi - \tan^{-1}\left(\frac{\omega^2 - 1}{2\omega\zeta}\right) \right) \quad (5.94)$$

for $j \in \mathbb{N}$ since \tan is 2π periodic. Note that $j = 0$ is not allowed since that would force $\tilde{\tau}$ to be negative. We then let $\Omega_j = 2\pi/\tilde{\tau}_j$ so that

$$\Omega_j = \frac{\omega\pi}{j\pi - \tan^{-1}\left(\frac{\omega^2 - 1}{2\zeta\omega}\right)}. \quad (5.95)$$

Equations 5.89 and 5.95 determines the boundary of the region of stability of the zero solution. This is shown in figure 5.10. For example, we consider the solution to equation 5.82 using $x(\tilde{t}) = 0.1, x'(\tilde{t}) = 0$ for $\tilde{t} \leq 0$, $\zeta = 0.1$ in the cases $\Omega = 1.5, p = 0.15, 0.3$ (marked in figure 5.10). From figure 5.10, we expect the solution in the $p = 0.15$ case to be stable and in the $p = 0.3$ case to be unstable. This is confirmed numerically in figure 5.11.

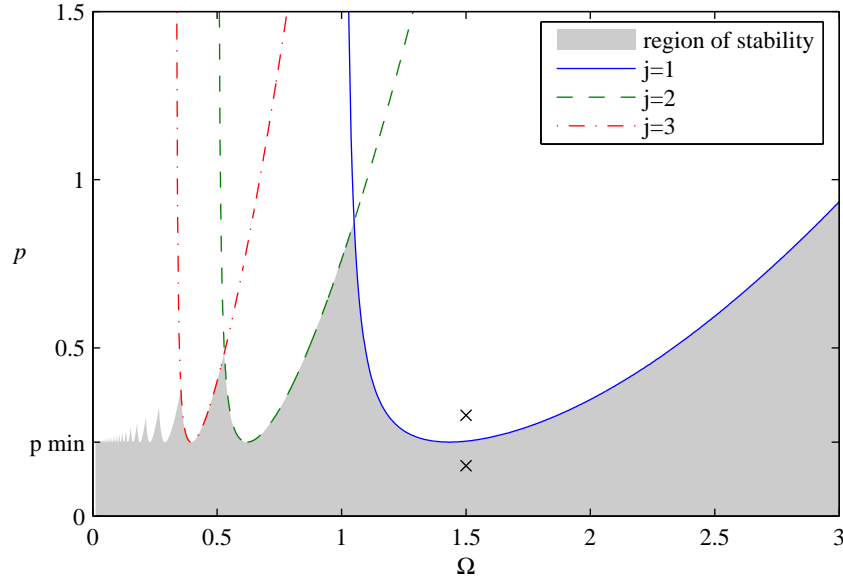


Figure 5.10: The region of stability of the zero solution of equation 5.82, as a function of p and Ω . We used $\zeta = 0.1$.

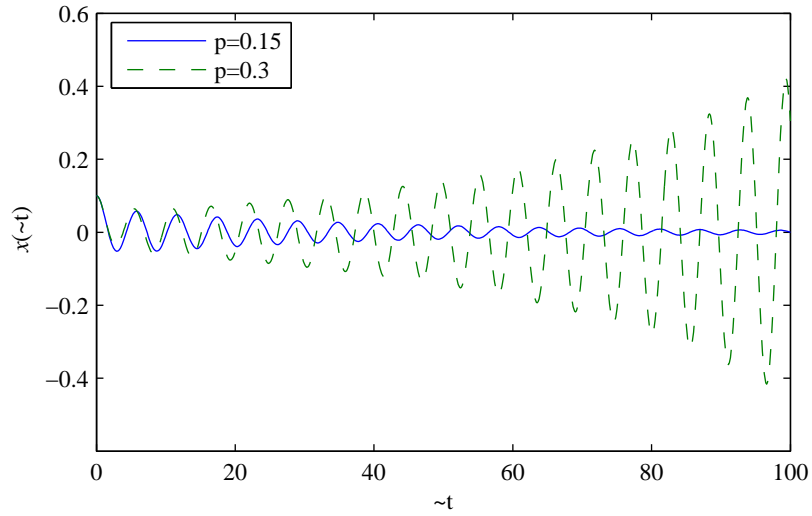


Figure 5.11: The solution to equation 5.82 using $x(\tilde{t}) = 0.1, x'(\tilde{t}) = 0$ for $\tilde{t} \leq 0$, $\zeta = 0.1$ and $\Omega = 1.5$. For $p = 0.15$ the solution is stable and for $p = 0.3$ the solution is unstable, as expected from figure 5.10. In this figure, $\sim t$ is used to denote \tilde{t} .

5.3 Car Following Model

Let us start by deriving the car following model as by Orosz et al. [19]. Consider n cars on a circular loop. If car i is at some position around the loop $x_i(t)$ at some time t then the distance in front of him is $x_{i+1}(t) - x_i(t)$ for $i = 1, \dots, n-1$ and $x_1(t) - x_n(t) + L$ for the last car. Now we assume that for a given distance $h_i(t)$ in front of car i , he would like to go at some speed $V(h_i(t))$. Moreover, we assume that the acceleration of car i is proportional to the difference between his desired speed and his actual speed,

$$\frac{d^2 x_i}{dt^2} = \alpha \left[V(h_i(t)) - \frac{dx_i}{dt} \right]. \quad (5.96)$$

In order to introduce the driver's reaction time, we suppose that the driver in fact determines his desired speed at some time slightly before the present, at time $t - \tau$. Our model is then

$$\frac{d^2 x_i}{dt^2} = \alpha \left[V(h_i(t - \tau)) - \frac{dx_i}{dt} \right]. \quad (5.97)$$

For a reasonable driver, there must be some nonzero distance h_{stop} such that for $h_i < h_{\text{stop}}$, the driver wishes to be stopped. Let us define a non-dimensional time $\tilde{t} \equiv t/\tau$ and a non-dimensional distance $\tilde{h} \equiv h/h_{\text{stop}}$. Then in terms of these new variables, our model becomes

$$\frac{h_{\text{stop}}}{\tau^2} \cdot \frac{d^2 \tilde{x}_i}{d\tilde{t}^2} = \alpha \left[\frac{h_{\text{stop}}}{\tau} \tilde{V}(\tilde{h}_i(\tilde{t} - 1)) - \frac{h_{\text{stop}}}{\tau} \frac{d\tilde{x}_i}{d\tilde{t}} \right] \quad (5.98)$$

$$\frac{d^2 \tilde{x}_i}{d\tilde{t}^2} = \alpha \tau \left[\tilde{V}(\tilde{h}_i(\tilde{t} - 1)) - \frac{d\tilde{x}_i}{d\tilde{t}} \right]. \quad (5.99)$$

Letting $\tilde{\alpha} \equiv \tau\alpha$ and removing the tildes, we obtain the final model

$$\begin{cases} \ddot{x}_i = \alpha [V(x_{i+1}(t-1) - x_i(t-1)) - \dot{x}_i] & i = 1, \dots, n-1 \\ \ddot{x}_n = \alpha [V(x_1(t-1) - x_n(t-1) + L) - \dot{x}_n], \end{cases} \quad (5.100)$$

where L is now the non-dimensionalised length of the circular loop. The non-dimensional $V(h_i)$ could be, for example,

$$V(h) = \begin{cases} 0 & \text{if } 0 \leq h \leq 1 \\ V_0 \frac{(h-1)^3}{1+(h-1)^3} & \text{if } h > 1 \end{cases} \quad (5.101)$$

This is shown in figure 5.12 for $V_0 = 1$. We now follow Orosz and Stépán [18]. The equilibrium solution is when all the cars are evenly spaced ($x_{i+1} - x_i = h^* \equiv \frac{L}{n}$) and travelling at constant speed $V^* = V(h^*)$. Then we have, without loss of generality, $x_i^{\text{eq}} = ih^* + V^*t$. If we let $\xi_i(t) = x_i(t) - x_i^{\text{eq}}(t)$, then equation 5.100 becomes, for $i = 1, \dots, n-1$,

$$\ddot{\xi}_i(t) = \alpha \left[V(\xi_{i+1}(t-1) - \xi_i(t-1) + h^*) - \dot{\xi}_i(t) - V^* \right]. \quad (5.102)$$

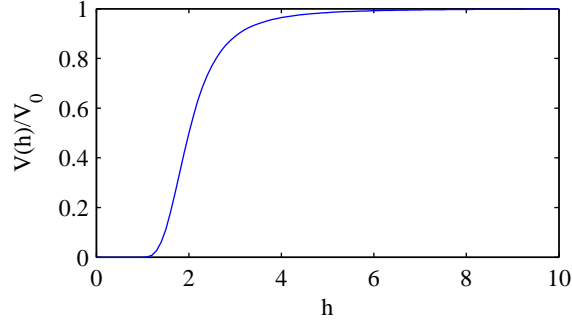


Figure 5.12: The speed function of a car in the car following model, as a function of h , the non-dimensionalised distance between two consecutive cars.

Approximating V by a Taylor series near h^* (i.e., for x_i near the stationary solution), we obtain

$$\begin{aligned} \ddot{\xi}_i(t) = \alpha \bigg[& V(h^*) + (\xi_{i+1}(t-1) - \xi_i(t-1)) V'(h^*) \\ & + (\xi_{i+1}(t-1) - \xi_i(t-1))^2 \frac{V''(h^*)}{2} \\ & + (\xi_{i+1}(t-1) - \xi_i(t-1))^3 \frac{V'''(h^*)}{6} - \dot{\xi}_i(t) - V^* \bigg] \end{aligned} \quad (5.103)$$

$$\begin{aligned} \ddot{\xi}_i(t) = -\alpha \dot{\xi}_i(t) + \alpha \bigg[& V(h^*) + (\xi_{i+1}(t-1) - \xi_i(t-1)) V'(h^*) \\ & + (\xi_{i+1}(t-1) - \xi_i(t-1))^2 \frac{V''(h^*)}{2} \\ & + (\xi_{i+1}(t-1) - \xi_i(t-1))^3 \frac{V'''(h^*)}{6} \bigg]. \end{aligned} \quad (5.104)$$

Doing likewise for x_n , we obtain

$$\begin{aligned} \ddot{\xi}_n = \alpha \big[& V(\xi_1(t-1) - \xi_n(t-1) + h^*) - \dot{\xi}_n(t) - V^* \big] \\ \ddot{\xi}_n = -\alpha \dot{\xi}_n(t) + \alpha \bigg[& V(h^*) + (\xi_1(t-1) - \xi_n(t-1)) V'(h^*) \end{aligned} \quad (5.105)$$

$$\begin{aligned} & + (\xi_1(t-1) - \xi_n(t-1))^2 \frac{V''(h^*)}{2} \\ & + (\xi_1(t-1) - \xi_n(t-1))^3 \frac{V'''(h^*)}{6} \bigg]. \end{aligned} \quad (5.106)$$

The linear approximation to equations 5.104 and 5.106 is

$$\begin{aligned} \ddot{\xi}_i &= -\alpha \dot{\xi}_i + \alpha V'(h^*) [\xi_{i+1}(t-1) - \xi_i(t-1)] \quad i = 1, \dots, n-1 \\ \ddot{\xi}_n &= -\alpha \dot{\xi}_n + \alpha V'(h^*) [\xi_1(t-1) - \xi_n(t-1)], \end{aligned} \quad (5.107)$$

to which zero is a solution. Letting $\xi_i = c_i e^{\lambda t}$, we obtain

$$\lambda^2 c_i = -\alpha \lambda c_i + \alpha V'(h^*) e^{-\lambda} (c_{i+1} - c_i) \quad (5.108)$$

$$\lambda^2 c_n = -\alpha \lambda c_n + \alpha V'(h^*) e^{-\lambda} (c_1 - c_n) \quad (5.109)$$

so that

$$(\lambda^2 + \alpha \lambda + \alpha V'(h^*) e^{-\lambda}) c_i = \alpha V'(h^*) e^{-\lambda} c_{i+1} \quad (5.110)$$

$$(\lambda^2 + \alpha \lambda + \alpha V'(h^*) e^{-\lambda}) c_n = \alpha V'(h^*) e^{-\lambda} c_1. \quad (5.111)$$

Rearranging, we then obtain that $rc_i = c_{i+1}$ for $i = 1, \dots, n-1$ and $rc_n = c_1$ where

$$r = \frac{\lambda^2 + \alpha \lambda + \alpha V'(h^*) e^{-\lambda}}{\alpha V'(h^*) e^{-\lambda}}. \quad (5.112)$$

As a result,

$$rc_i = c_{i+1} \quad (5.113)$$

$$r^{n-1} c_1 = c_n \quad (5.114)$$

$$r^{n-1} (rc_n) = c_n \quad (5.115)$$

$$r^n = 1 \quad (5.116)$$

$$r^n = e^{2\pi i k} \quad (5.117)$$

$$r = e^{2\pi i k/n} \quad (5.118)$$

$$\lambda^2 + \alpha \lambda + \alpha V'(h^*) e^{-\lambda} = \alpha V'(h^*) e^{-\lambda} e^{2\pi i k/n}, \quad (5.119)$$

which is our characteristic equation. If we let $\lambda = p + iq$, by equating real and imaginary parts, we obtain that

$$p^2 - q^2 + \alpha p = -2\alpha V'(h^*) e^{-p} \sin\left(\pi \frac{k}{n}\right) \sin\left(\pi \frac{k}{n} - q\right) \quad (5.120)$$

$$2pq + \alpha q = 2\alpha V'(h^*) e^{-p} \sin\left(\pi \frac{k}{n}\right) \cos\left(\pi \frac{k}{n} - q\right). \quad (5.121)$$

From this, we can solve for α and $V'(h^*)$ in terms of p , q and k/n . Letting those parameters vary, with the constraint that $p > 0$, we obtain the region in which there is an unstable solution. As a result, we can determine the region of stability. This is plotted as a function of α and $V'(h^*)$ in figure 5.13. Observe that we obtain stability for small values of $V'(h^*)$, which corresponds to drivers that only change their speed a little bit when the space in front of them changes by a little bit near the equilibrium spacing, h^* . We also obtain stability for large values of α , which corresponds to slow reaction time of the drivers. In addition, as the reaction time of the drivers, α , increases, this allows for stability for larger values of $V'(h^*)$ (i.e., larger variations in speed near the equilibrium driving spacing).

Orosz and Stépán [18] determine that this model exhibits a subcritical Hopf bifurcation. As a result, in the region in parameter-space where the stationary

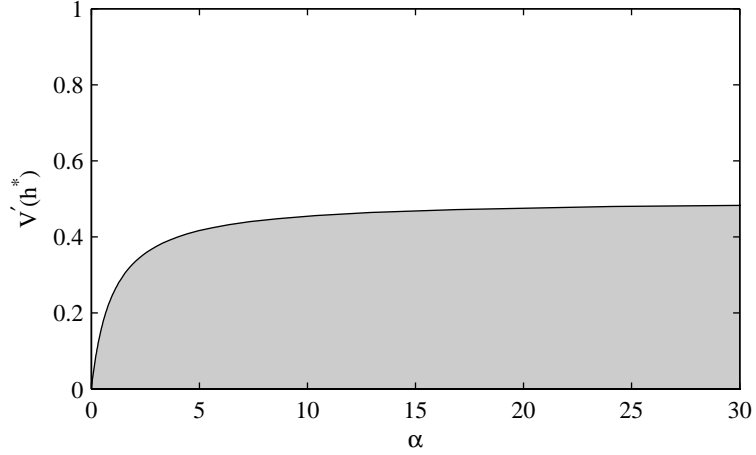


Figure 5.13: The region of stability of the stationary solution, as a function of α and $V'(h^*)$, in the approximation for n large, so $k/n \ll 1$.

solution is stable, we expect there to also be an unstable oscillatory solution. As an example, we compute numerically using MATLAB the solution to equation 5.104 for a few different values of the parameters. First, we calculate the solution using $\alpha = 1, h^* = 2.3, n = 2$. This is shown in figure 5.14, with two different initial conditions. In this figure, the origin is stable and we can see an unstable circular orbit around it. We also calculate the solution using $\alpha = 1, h^* = 2.1, n = 2$. This is shown in figure 5.15. Here, the origin is now unstable. Note that there is also a stable circular orbit. This is perhaps that predicted by Orosz and Stépán [18]. For our choice of $V(h)$, $h^* = 2.1$ corresponds to $V'(h^*) = 0.67$ and $h^* = 2.3$ corresponds to $V'(h^*) = 0.50$. We construct the $n = 1$ version of figure 5.13, shown in figure 5.16. From this, we predict, that $\alpha = 1, h^* = 2.1$ will have an unstable origin and $\alpha = 1, h^* = 2.3$ will have a stable origin. This is precisely what is observed.

5.4 Band-Limited Feedback

Consider a simple circuit which consists of two devices: a band-pass filter and a nonlinear feedback G with some amplification γ and some delay T . For this, we will follow Illing and Gauthier [11]. The model is

$$\frac{dz_1}{dt} = -\frac{z_1}{\tau_h} + \frac{dz_2}{dt}, \quad (5.122)$$

$$\tau_l \frac{dz_2}{dt} = -z_2 + \gamma G[z_1(\tilde{t} - T)], \quad (5.123)$$

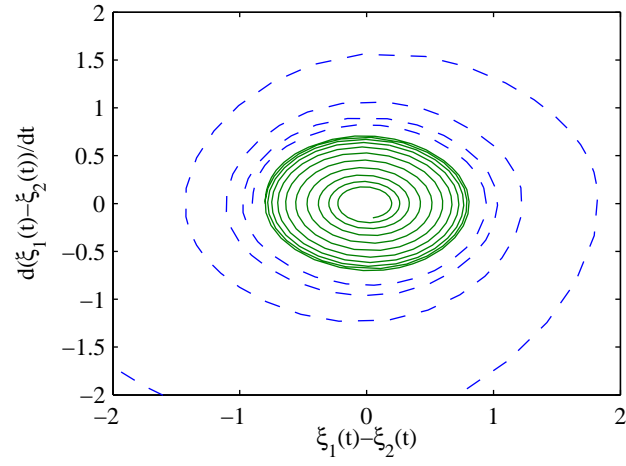


Figure 5.14: Two simulations of equation 5.104 with $\alpha = 1, h^* = 2.3, n = 2$ and different initial conditions, showing the stable origin and unstable oscillatory solution.

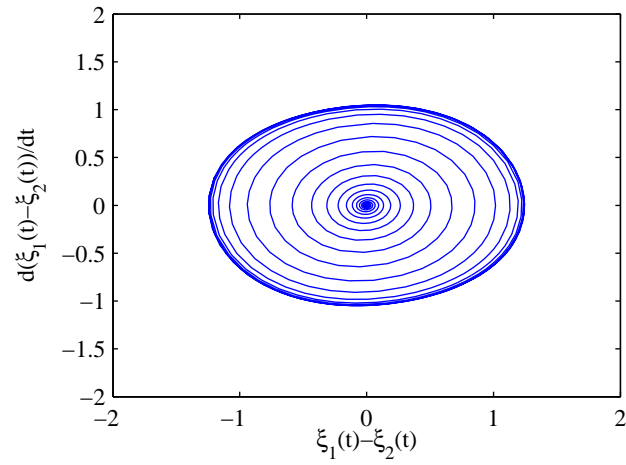


Figure 5.15: A simulation of equation 5.104 with $\alpha = 1, h^* = 2.1, n = 2$, showing the unstable origin.

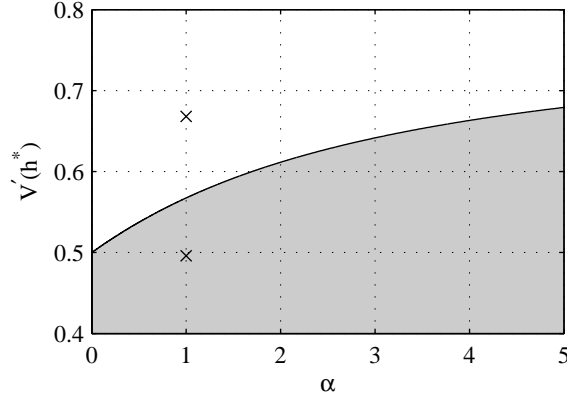


Figure 5.16: The region of stability of the stationary solution, as a function of α and $V'(h^*)$, for $n = 1$.

where τ_l and τ_h are the periods corresponding to the low and high frequency cutoffs of the band-pass filter. If we let

$$t = \tilde{t} \left(\frac{1}{\tau_l} + \frac{1}{\tau_h} \right), \quad x = z_1, \quad y = \frac{\tau_h}{\tau_h + \tau_l} (z_1 - z_2 + \gamma G[0]) \quad (5.124)$$

and substitute this into the above equations, we obtain

$$\frac{dy}{dt} = \frac{\tau_l \tau_h}{(\tau_l + \tau_h)^2} x \quad (5.125)$$

$$\frac{dx}{dt} = -x + y + \gamma \frac{\tau_h}{\tau_l + \tau_h} \left(G \left[x \left(t - T \frac{\tau_l + \tau_h}{\tau_l \tau_h} \right) \right] - G[0] \right) \quad (5.126)$$

which combine to give

$$\ddot{x} = -\dot{x} - rx + \gamma f'(x(t - \tau)) \dot{x}(t - \tau) \quad (5.127)$$

where we have defined

$$\tau \equiv T \frac{\tau_l + \tau_h}{\tau_l \tau_h} \quad (5.128)$$

$$r \equiv \frac{\tau_l \tau_h}{(\tau_l + \tau_h)^2}. \quad (5.129)$$

Observe that $x = 0$ is a solution to this. Near this solution, $f'(x(t - \tau)) \simeq f'(0)$, so let $b \equiv \gamma f'(0)$ so that

$$\ddot{x} = -\dot{x} - rx + b \dot{x}(t - \tau). \quad (5.130)$$

In order to determine the stability of the zero solution, as usual we let $x = \exp(\lambda t)$, and we obtain

$$\lambda^2 = -\lambda - r + b \lambda e^{-\lambda \tau}. \quad (5.131)$$

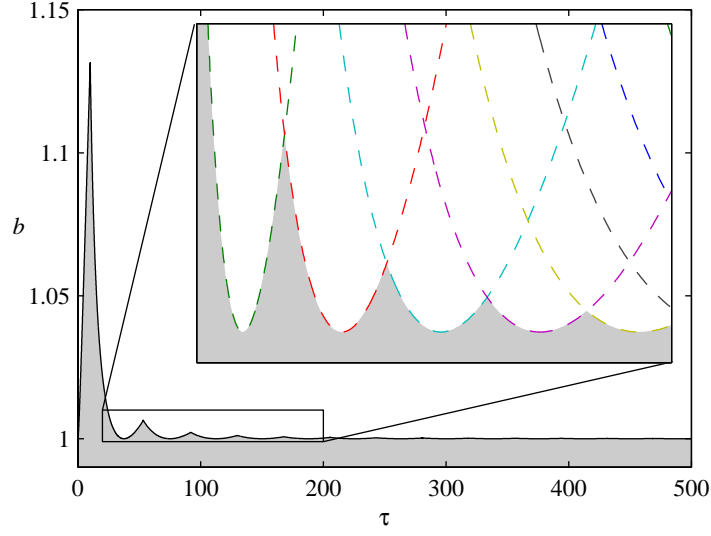


Figure 5.17: The region of stability of the band-limited feedback model.

Letting $\lambda = i\omega$ and equating real and imaginary parts, this gives

$$b = \frac{1}{\cos(\omega\tau)} \quad (5.132)$$

$$\tau = \frac{\omega\tau}{2r} \left(\tan(\omega\tau) + \sqrt{\tan^2(\omega\tau) + 4r} \right). \quad (5.133)$$

Parameterising these by $\omega\tau$, we obtain the lines shown in the inset in figure 5.17. Each individual line corresponds to

$$-\frac{\pi}{2} + 2\pi k \leq \omega\tau \leq \frac{\pi}{2} + 2\pi k \quad (5.134)$$

for a different value of k . The lines corresponding to

$$\frac{\pi}{2} + 2\pi k \leq \omega\tau \leq \frac{3\pi}{2} + 2\pi k \quad (5.135)$$

are as those shown, except mirrored across the τ -axis. The region of stability is then the region shaded in figure 5.17.

5.5 Lindstedt's Method

For this section, we follow the example given by Rand [23]. Consider the example

$$\frac{dx}{dt} = -x(t-T) - x(t)^3. \quad (5.136)$$

Let $\tau = \omega t$ so that

$$\omega \frac{dx(\tau)}{d\tau} = -x(\tau - \omega T) - x(\tau)^3. \quad (5.137)$$

Now it can be shown that a bifurcation occurs at $T = \pi/2$, so let $T = \pi/2 + \epsilon\mu$ and $x = \sqrt{\epsilon}u$. Then

$$\omega \frac{du}{d\tau} = -u \left(\tau - \omega \left(\frac{\pi}{2} + \epsilon\mu \right) \right) - \epsilon u^3. \quad (5.138)$$

Expanding u and ω by

$$u(\tau) = u_0(\tau) + \epsilon u_1(\tau) + \dots \quad \omega = 1 + \epsilon k_1 + \dots, \quad (5.139)$$

we obtain that

$$u \left(\tau - \frac{\pi}{2} - \epsilon \left(k_1 \frac{\pi}{2} + \mu \right) \right) = u \left(\tau - \frac{\pi}{2} \right) - \epsilon \left(k_1 \frac{\pi}{2} + \mu \right) \frac{du}{d\tau} \left(\tau - \frac{\pi}{2} \right) + \dots \quad (5.140)$$

Using this in equation 5.138 and equating terms of equal order, we obtain

$$\frac{du_0}{d\tau} = -u_0 \left(\tau - \frac{\pi}{2} \right) \quad (5.141)$$

so without loss of generality, we can choose $u_0 = A \cos(\tau)$. Terms of order ϵ in equation 5.138 give us

$$\begin{aligned} \frac{du_1}{d\tau} + u_1 \left(\tau - \frac{\pi}{2} \right) &= k_1 A \sin(\tau) + \left(k_1 \frac{\pi}{2} + \mu \right) A \cos(\tau) \\ &\quad - A^3 \left(\frac{3}{4} \cos(\tau) + \frac{1}{4} \cos(3\tau) \right), \end{aligned} \quad (5.142)$$

which we can write as

$$\frac{du_1}{d\tau} + u_1 \left(\tau - \frac{\pi}{2} \right) = \alpha \sin(\tau) + \beta \cos(\tau) - \frac{A^3}{4} \cos(3\tau). \quad (5.143)$$

Now consider the solution to this on some interval $[0, 2\pi k]$. In that interval, provided $u_1(\tau)$ is piecewise continuous, we can always write

$$u_1(\tau) = \sum_{n=0}^{\infty} \left(a_n \sin \left(\frac{n\tau}{k} \right) + b_n \cos \left(\frac{n\tau}{k} \right) \right) \quad (5.144)$$

so that equation 5.143 becomes

$$\begin{aligned} \sum_{n=0}^{\infty} \left[a_n \frac{n}{k} \cos \left(\frac{n}{k} \tau \right) - b_n \frac{n}{k} \sin \left(\frac{n}{k} \tau \right) \right. \\ \left. + a_n \cos \left(\frac{n\pi}{2k} \right) \sin \left(\frac{n}{k} \tau \right) - a_n \sin \left(\frac{n\pi}{2k} \right) \cos \left(\frac{n}{k} \tau \right) \right. \\ \left. + b_n \cos \left(\frac{n\pi}{2k} \right) \cos \left(\frac{n}{k} \tau \right) + b_n \sin \left(\frac{n\pi}{2k} \right) \sin \left(\frac{n}{k} \tau \right) \right] \\ = \alpha \sin(\tau) + \beta \cos(\tau) - \frac{A^3}{4} \cos(3\tau). \end{aligned} \quad (5.145)$$

We now use orthogonality. By equating the coefficients of $\sin(\tau)$ we obtain that $\alpha = 0$, and by equating the coefficients of $\cos(\tau)$ we obtain that $\beta = 0$. Note that this does not tell us what a_k and b_k are. By equating the coefficients of $\sin(3\tau)$ we obtain that $b_{3k} = 0$, and by equating the coefficients of $\cos(3\tau)$ we obtain that $a_{3k} = -A^3/16$. For other values of k , by equating the coefficients of $\sin(n\tau/k)$ and $\cos(n\tau/k)$, we obtain

$$b_n \frac{n}{k} = a_n \cos\left(\frac{n\pi}{2k}\right) + b_n \sin\left(\frac{n\pi}{2k}\right) \quad (5.146)$$

$$a_n \frac{n}{k} = a_n \sin\left(\frac{n\pi}{2k}\right) - b_n \cos\left(\frac{n\pi}{2k}\right), \quad (5.147)$$

so that

$$(a_n^2 + b_n^2) \left(\left(\frac{n}{k} \right)^2 - 1 \right) = 0. \quad (5.148)$$

Since by assumption $n \neq k$, then we must have $a_n = b_n = 0$ for all $n \neq k, 3k$.

Note that since we determined we must have

$$0 = \beta \equiv Ak_1, \quad (5.149)$$

we must have $k_1 = 0$. Also, since

$$0 = \alpha \equiv A \left(k_1 \frac{\pi}{2} + \mu - A^2 \frac{3}{4} \right), \quad (5.150)$$

then $A = 2\sqrt{\mu/3}$. So we have found that (assuming $a_k = b_k = 0$)

$$u(\tau) = u_0(\tau) + \epsilon u_1(\tau) \quad (5.151)$$

$$u(\tau) = \frac{2}{\sqrt{3}} \sqrt{\mu} \cos(\tau) - \frac{1}{16\sqrt{\epsilon}} \left(\frac{2}{\sqrt{3}} \sqrt{\mu\epsilon} \right)^3 \sin(3\tau) \quad (5.152)$$

$$x(\tau) = \frac{2}{\sqrt{3}} \sqrt{\mu\epsilon} \cos(\tau) - \frac{1}{16} \left(\frac{2}{\sqrt{3}} \sqrt{\mu\epsilon} \right)^3 \sin(3\tau) \quad (5.153)$$

$$x(\tau) \equiv \Lambda_0 \cos(\tau) + \Lambda_1 \sin(3\tau) \quad (5.154)$$

where

$$\mu\epsilon = T - \frac{\pi}{2}. \quad (5.155)$$

For $T = \pi/2 + 0.01$, we then expect $\Lambda_0 = 0.1155, \Lambda_1 = -9.62 \times 10^{-5}$. Using MATLAB to simulate the delay differential equation and gnuplot to extract the amplitude, we determine numerically that $\Lambda_0 = 0.1149, \Lambda_1 = -9.49 \times 10^{-5}$. These are shown in table 5.1. Note that it is very difficult to determine these values precisely, so some of the trailing digits in the numerical values may be incorrect, especially for $\omega = 1$. Now if we use the same method as above, but write $\omega \equiv 1 + \epsilon\kappa_1$ where κ_1 is assumed to be known, then we obtain

$$\Lambda_0 = \frac{2}{\sqrt{3}} \sqrt{\mu\epsilon + \epsilon\kappa_1} \frac{\pi}{2}. \quad (5.156)$$

	$\omega - 1 = \epsilon\kappa_1$	Λ_0	Λ_1
numerical	-5.7280×10^{-5}	0.114946	-9.4926×10^{-5}
theoretical	0	0.115470	-9.6225×10^{-5}
modified theoretical	(-5.7280×10^{-5})	0.114949	-9.4929×10^{-5}

Table 5.1: A comparison between the stationary solution under different approximations.

Using this, together with $\Lambda_1 = -\Lambda_0^3/16$ and the numerical value for κ_1 , we obtain the values listed in table 5.1 under the title ‘modified theoretical’. Note that these agree very well with the numerical values.